RSC Advances

PAPER

View Article Online
View Journal | View Issue

Cite this: *RSC Adv.*, 2024, **14**, 16083

Development of phenyllactic acid ionic liquids and evaluation of cytotoxicity to human cervical epithelial cells†

Phoebe Crossley, ‡[ad] Yogesh Sutar,‡[b] Irina Tsoy,[b] Srushti Mukkirwar,[b] Paweł Łaniewski,[c] Melissa M. Herbst-Kralovetz *[cde] and Abhijit A. Date *[bef]

Phenyllactic acid (PLA), is a naturally produced, broad-spectrum antimicrobial compound with activity against bacteria and fungi. PLA can be produced by a variety of lactic acid bacteria, including vaginal *Lactobacillus* species, which are healthy constituents of the vaginal microbiome with a protective role against invading pathogenic bacteria and/or fungi. Additionally, PLA has been shown to exhibit anti-inflammatory and immunomodulatory properties, overall indicating its therapeutic potential as an intravaginally delivered compound for modulation of the vaginal microbiome. However, PLA has low kinetic solubility in water. Hence, strategies to improve the solubility of PLA are necessary to facilitate its intravaginal delivery. Using biocompatible cations, choline and carnitine, we successfully transformed both D- and L-enantiomers of crystalline PLA into amorphous low-melting ionic liquids (ILs) with high water solubility. We further evaluated the *in vitro* cytotoxicity of PLA ILs to human cervical epithelial cells. Microscopic visualisation of cellular morphology using crystal violet staining and MTT cell proliferation assay revealed that PLA ILs result in minimal morphological changes and low cytotoxicity to human cervical epithelial cells. Overall, we successfully demonstrated that transforming PLA into ILs efficiently enhances its solubility in water and these formulations are not toxic to human epithelial cells. This investigation lays the groundwork for future testing of PLA ILs for their antimicrobial properties and metabolic activity within the cervicovaginal microenvironment.

Received 9th March 2024
Accepted 24th April 2024

DOI: 10.1039/d4ra01812e

rsc.li/rsc-advances

Introduction

Phenyllactic acid (3-phenyllactic acid or 2-hydroxy-3-phenylpropanoic acid; PLA) is an organic phenolic acid, naturally found in honey and foods and produced by lactic acid bacteria (LAB).[1] It is a common metabolite of many LABs, including *Lactobacillus* species, which are widely found in the healthy microbiomes of the human gut,[2] bladder,[3] and vagina.[4] This metabolite gained significant interest as a "green preservative" in the food industry[5,6] owing to its natural broad-spectrum antimicrobial activity against bacteria[7–10] and fungi.[11,12] PLA exists in two optical isomeric forms known as enantiomers, D-PLA and L-PLA, with D-PLA demonstrating greater antimicrobial activity than L-PLA.[13] Beyond the food industry, PLA has been researched for vast applications in agriculture,[14] pharmaceutical,[15] and cosmetic[16] industries. In addition, PLA has been investigated in the biomedical field, where it has demonstrated beneficial metabolic functions, including immunomodulatory[17] and anti-inflammatory activity.[18]

Recently, we discovered that commensal vaginal *Lactobacillus* species, including *Lactobacillus crispatus*, *Lactobacillus paragasseri*, and *Lactobacillus iners*, were capable of producing PLA *in vitro*.[19,20] Within the lower female reproductive tract, it is well established that microbiota dominated by *Lactobacillus* spp. provide protection against pathogenic diseases, such as sexually transmitted infections,[21,22] urinary tract infections,[23] and bacterial vaginosis.[24,25] *Lactobacilli* achieve this by producing lactic acid to maintain an acidic microenvironment.[26] However, the role of other metabolites produced by lactobacilli, such as PLA and other aromatic lactic acids, is still not well-known. An *in vitro* study showed that PLA is produced by a bladder isolate of *L. crispatus* and exhibits antimicrobial properties against Gram-positive, Gram-negative, and fungal urogenital pathogens, such as *Streptococcus agalactiae* (also

[a]*Department of Life Sciences, University of Bath, Bath, UK*
[b]*Department of Pharmacology and Toxicology, R. Ken Coit College of Pharmacy, University of Arizona, Tucson, AZ, USA. E-mail: abhijitdate@arizona.edu*
[c]*Department of Basic Medical Sciences, College of Medicine – Phoenix, University of Arizona, Phoenix, AZ, USA. E-mail: mherbst1@arizona.edu*
[d]*Department of Obstetrics and Gynecology, College of Medicine – Phoenix, University of Arizona, Phoenix, AZ, USA*
[e]*University of Arizona Cancer Center, University of Arizona, Tucson, AZ, USA*
[f]*Department of Ophthalmology and Visual Sciences, University of Arizona College of Medicine, Tucson, AZ, USA*

† Electronic supplementary information (ESI) available. See DOI: https://doi.org/10.1039/d4ra01812e

‡ Authors contributed equally.

known as Group B *Streptococcus*), *Klebsiella pneumoniae*, and *Candida albicans*.[27] PLA's broad-spectrum antimicrobial properties, potential immunomodulatory functions, and its natural production in the cervicovaginal microenvironment demonstrate its promising applications as an intravaginally delivered compound to maintain mucosal homeostasis in the lower female reproductive tract. However, PLA has low kinetic solubility in water, and it requires toxic solvents such as dimethyl sulfoxide (DMSO) for the solubilisation of high quantities of PLA. As DMSO cannot be used for vaginal delivery, a solubilisation strategy that uses biocompatible ingredients to solubilise high quantities of PLA for intravaginal delivery is required.

Ionic liquids (ILs) are organic salts, composed solely of cations and anions, with melting points lower than 100 °C. In the past few years, ILs have received great attention in the pharmaceutical and biomedical sciences as a novel delivery strategy to improve the solubility, permeability, and bioavailability of ionizable compounds.[28,29] We hypothesised that anionic PLA can interact with biocompatible cations to yield biocompatible and highly soluble PLA ILs suitable for delivery to various mucosal surfaces including the vagina.

In this study, we demonstrated that crystalline PLA can be transformed into amorphous ionic liquids (PLA ILs), using cations of natural origin (choline and carnitine), that have ~55-fold higher water solubility compared to D- and L-PLA. We further conducted preliminary *in vitro* cytotoxicity testing of these PLA ILs on human cervical epithelial cells to determine their safety.

Methods

Materials

D-PLA and L-PLA were purchased from TCI Chemicals (Portland, OR, USA). Choline bicarbonate was obtained from Sigma-Aldrich (St. Louis, MO, USA). L-Carnitine free base was purchased from Spectrum Chemical (Gardena, CA, USA). Methanol (analytical reagent grade) was purchased from VWR International (Radnor, PA, USA). All other chemicals used were of analytical grade unless otherwise indicated.

High-pressure liquid chromatography method for PLA

To evaluate the purity of the synthesized D- or L-PLA ILs and for the determination of their water solubility, a reverse phase-HPLC method was developed. The HPLC apparatus consisted of a Shimadzu LC2050C-3D system with a PDA detector. Samples were run through a C_{18} precolumn and a Gemini C_{18} reverse-phase column [150 × 4.5 mm (I.D.)] with 5 μm particle size packing (Phenomenex, Torrance, CA). The mobile phase contained acetonitrile and 20 mM phosphoric acid solution in water (25 : 75). The flow rate of the mobile phase was set at 0.8 mL min^{-1}, the column oven was set at 45 °C, the injection volume was 10 μL, and the detection was carried out at 210 nm. The retention time for PLA was 5.5 min. For the standard curve, D- or L-PLA stock solutions (0.1 mg mL^{-1}) were prepared in methanol. The stock solutions were diluted to obtain solutions of various concentrations. The standard curve was obtained by injecting 5–25 μg mL^{-1} of PLA. All the experiments were performed in triplicate.

Synthesis of Chol : D-PLA and Chol : L-PLA ILs

For the transformation of D-PLA and L-PLA into IL, choline bicarbonate (Chol; 80 wt% solution, 0.605 mmol) was added dropwise to the D-PLA and L-PLA (0.605 mmol for 1 : 1 molar ratio; 1.210 mmol for 1 : 2 molar ratio) in an open round bottom flask. The mixture was stirred at room temperature until the CO_2 effervescence stopped. After that, the mixture was dried on a rotary evaporator at 60 °C for 1–2 h to remove water followed by drying in a vacuum oven for 2 days to obtain a clear viscous liquid product (yield: 98%).

Chol : D-PLA (1 : 1). ^{1}H NMR (500 MHz, DMSO-d_6) δ 7.24–7.08 (m, 5H), 6.25 (s, 1H), 4.40 (s, 1H), 4.05 (s, 1H), 3.85 (d, J = 4.6 Hz, 1H), 3.63 (d, J = 8.5 Hz, 1H), 3.41 (dd, J = 8.6, 3.6 Hz, 2H), 3.11 (s, 9H), 2.99 (dd, J = 13.7, 3.1 Hz, 1H), 2.53–2.48 (m, 1H). ^{13}C NMR (500 MHz, DMSO-d_6) δ 175.72, 141.08, 129.50, 127.82, 125.45, 72.43, 67.28, 55.25, 53.32, 41.44.

Chol : D-PLA (1 : 2). ^{1}H NMR (500 MHz, DMSO-d_6) δ 7.28–7.13 (m, 10H), 5.61 (s, 2H), 3.92 (dd, J = 8.6, 3.7 Hz, 2H), 3.84 (dq, J = 5.0, 2.6 Hz, 2H), 3.42–3.39 (m, 2H), 3.10 (s, 8H), 2.99 (dd, J = 13.7, 3.7 Hz, 2H), 2.64 (dd, J = 13.7, 8.6 Hz, 2H). ^{13}C NMR (500 MHz, DMSO-d_6) δ 175.96, 139.80, 129.55, 127.96, 125.82, 71.96, 67.23, 55.28, 53.34, 40.81.

Chol : L-PLA (1 : 1). ^{1}H NMR (500 MHz, DMSO-d_6) δ 7.28–7.01 (m, 5H), 6.48 (s, 1H), 4.36 (s, 1H), 3.85 (q, J = 5.4 Hz, 2H), 3.72–3.65 (m, 1H), 3.44–3.40 (m, 2H), 3.12 (s, 9H), 3.00 (dd, J = 13.7, 3.1 Hz, 1H), 2.55–2.50 (m, 1H). ^{13}C NMR (500 MHz, DMSO-d_6) δ 175.99, 140.96, 129.53, 127.86, 125.52, 72.47, 67.28, 55.26, 53.26, 41.43.

Chol : L-PLA (1 : 2). ^{1}H NMR (500 MHz, DMSO-d_6) δ 7.25–7.14 (m, 10H), 5.64 (s, 2H), 3.91 (dd, J = 8.5, 3.6 Hz, 2H), 3.86–3.81 (m, 2H), 3.40 (dd, J = 6.7, 3.4 Hz, 2H), 3.10 (s, 9H), 2.99 (dd, J = 13.7, 3.6 Hz, 2H), 2.64 (dd, J = 13.7, 8.6 Hz, 2H). ^{13}C NMR (500 MHz, DMSO-d_6) δ 175.72, 139.61, 129.37, 127.79, 125.66, 71.77, 67.00, 55.11, 53.11, 40.62.

Synthesis of Car : D-PLA and Car : L-PLA ILs

An equimolar quantity (0.620 mmol) of L-carnitine (Car) and D-PLA or L-PLA were dissolved in 10 mL of methanol. The mixture was stirred on a magnetic stirrer for 3 h at room temperature. After that, the mixture was concentrated on a rotary evaporator to obtain clear viscous liquid (yield: 99%).

Car : D-PLA. ^{1}H NMR (500 MHz, DMSO-d_6) δ 7.31–7.07 (m, 5H), 5.58 (s, 2H), 4.36 (p, J = 6.4 Hz, 1H), 3.90 (dd, J = 8.5, 3.7 Hz, 1H), 3.35–3.29 (m, 2H), 3.12 (s, 9H), 2.99 (dd, J = 13.7, 3.6 Hz, 1H), 2.63 (dd, J = 13.7, 8.6 Hz, 1H), 2.31–2.21 (m, 2H). ^{13}C NMR (500 MHz, DMSO-d_6) δ 176.12, 172.95, 139.85, 129.56, 127.96, 125.82, 72.00, 70.09, 63.07, 53.59, 41.25, 40.84.

Car : L-PLA. ^{1}H NMR (500 MHz, DMSO-d_6) δ 7.27–7.14 (m, 5H), 6.58 (s, 2H), 4.36 (p, J = 6.8 Hz, 1H), 3.91 (dd, J = 8.6, 3.7 Hz, 1H), 3.33 (d, J = 3.7 Hz, 2H), 3.12 (s, 9H), 2.99 (dd, J = 13.7, 3.6 Hz, 1H), 2.64 (dd, J = 13.7, 8.6 Hz, 1H), 2.31–2.22 (m, 2H). ^{13}C NMR (500 MHz, DMSO-d_6) δ 175.95, 172.76, 139.67, 129.39, 127.79, 125.65, 71.82, 69.91, 62.89, 53.41, 41.09, 40.66.

Fourier-transform infrared (FT-IR) spectroscopy

The FTIR spectroscopy measurements were conducted on a Nicolet iS10 Fourier-Transform Infrared (FTIR) Spectrophotometer (Thermo Scientific, Waltham, MA) with a diamond attenuated total reflection (ATR) unit. FTIR spectra were obtained in '% transmission' mode from 4000 to 500 cm^{-1} with an average of 16 scans for obtaining background.

Nuclear magnetic resonance (NMR) spectroscopy

NMR spectra were obtained using a Bruker Avance Digital 500 MHz NMR spectrometer (Bruker Corp., Billerica, MA) and an automatic sample changer, the BACS1. A 5 mm PABBO BB-1H/D Z-GRD probe was mounted onto the spectrometer. The ^{13}C spectrum of each sample was recorded using an average of 1000 scans, and the ^{1}H spectrum of the refined products (6–8 mg) was obtained using an average of 16 scans in dimethyl sulfoxide-d_6 (Cambridge Isotope Laboratories, Inc., Tewksbury, MA). Chemical changes were reported in parts per million (ppm) units.

Thermogravimetric analysis (TGA)

TA Instruments Discovery TGA 5500 (TA instruments, New Castle, DE, USA) was used to analyse pure PLA, carnitine, and various PLA ILs. The samples were accurately weighed (2–5 mg) in platinum pans and placed onto the autosampler. The samples were heated from 30 °C to 350 °C at 10 °C min^{-1}; nitrogen was purged at a rate of 25 mL min^{-1}. TRIOS software (TA instruments, New Castle, DE, USA) was used to analyse the data.

Differential scanning calorimetry (DSC)

The TA Instruments DSC 2500 RCS40 cooling unit (TA instruments, New Castle, DE, USA), calibrated with indium, was used to record thermograms of pure compounds of D-PLA, L-PLA, carnitine, and their corresponding ILs. The samples were weighed (6–10 mg) and hermetically sealed in T_{zero} aluminium pans, along with an empty reference T_{zero} pan. The atmosphere was inert because of nitrogen purge at a rate of 25 mL min^{-1}. The samples were heated from 30 °C to the temperature equivalent to a 5% weight loss point with a 5 °C min^{-1} ramp for each sample to observe thermal transitions. The glass transition temperature (T_g) for each sample was recorded in the cool/heat run at 5 °C min^{-1} ramp from 30 °C to −80 °C, and from −80 °C to 30 °C. TRIOS software (TA instruments, New Castle, DE, USA) was used to analyse the data.

Powder X-ray diffraction (PXRD) spectroscopy

The crystallinity of samples was assessed using a Philips PANalytical X'Pert PRO MPD (Malvern Panalytical, Malvern, UK) with a copper X-ray source (Kα radiation with $\lambda = 1.5406$ Å). The PLA, carnitine, or PLA ILs were placed into a 20 × 20 mm sample holder pocket that was 0.2 mm deep and the surface was leveled. The diffraction pattern of the samples was acquired at room temperature by scanning across a range of 5.0 to 70.0° (2θ) at a speed of 0.63° per second.

Equilibrium solubility and pH determination studies

The equilibrium solubility of D-PLA, L-PLA, and their ILs was determined using a previously reported method.[30] An excess amount of D-PLA, L-PLA, or their ILs was added in an Eppendorf tube containing 1 mL of water. The samples were placed on an orbital shaker set at a speed of 200 rpm and were equilibrated at room temperature for 24 h. After 24 h, the samples were centrifuged, the supernatant was filtered using a 0.22 μm syringe filter and further diluted using methanol as necessary. The D-PLA or L-PLA content in the supernatant was analyzed using the HPLC method to calculate the equilibrium solubility. Further, the pH values of D-PLA, L-PLA, and their ILs dissolved in water were determined using a VWR 1100L pH meter.

Human endocervical epithelial cell culture

Human endocervical epithelial cell line (A2EN), generated from human endocervical explant tissue,[31] was cultured as monolayers in keratinocyte serum-free medium (KFSM) supplemented with recombinant epidermal growth factor (5 ng mL^{-1}), bovine pituitary extract (50 μg mL^{-1}; Gibco), $CaCl_2$ (22 mg mL^{-1}; Sigma-Aldrich), and primocin (100 μg mL^{-1}; InvivoGen, San Diego, CA), herein referred to as A2 medium, at 37 °C under 5% carbon dioxide (CO_2) atmosphere.

Preparation of PLA ILs and pH solutions

Prior to cytotoxicity testing, PLA ILs were diluted to 1 M concentrations with distilled water and filtered using a sterile 0.2 μm syringe filter. Solutions with pH ranging from 4 to 7.5 were prepared by adjusting the pH of A2 media with hydrochloric acid (HCl), following filtration using a sterile 0.2 μm syringe filter.

Crystal violet staining for cervical cell morphology

Cervical cell morphology following PLA IL treatment was visualised using 2.3% crystal violet stain with 0.1% ammonium oxalate and 20% ethanol (Sigma-Aldrich). Cervical cell monolayers were seeded into a tissue-treated 24-well microtiter plate (Falcon) at a density of 1.5×10^5 cells per well and incubated for 24 h at 37 °C under 5% CO_2. Two-fold serial dilutions of each PLA IL were prepared and aliquoted into respective wells to obtain final concentrations of 3.125 to 100 mM. Deionised water and 1% conceptrol (v/v), containing the detergent, nonoxynol-9, were used as negative and positive controls, respectively. Following 24 h incubation at 37 °C under 5% CO_2 atmosphere, adhered cells were stained with 100 μL of crystal violet for 5 minutes, washed thoroughly with deionised water until clear, and imaged at 10× magnitude using a bright-field microscope (Olympus IX71). HCl solutions (with pH ranging from 4 to 7.5) were also tested for cell morphology changes following the same protocol.

MTT assay for cervical cell proliferation

Cervical cell monolayers were seeded into a tissue-treated 96-well microtiter plate (Corning Costar) at a density of 2.0×10^4 cells per well and incubated for 24 h at 37 °C under 5% CO_2.

Cells were treated with each PLA IL at concentrations ranging from 3.125 to 100 mM and incubated for 24 h (37 °C under 5% CO_2). MTT [3-(4,5-dimethylthiazol-2-yl)-2,5-diphenyltetrazolium bromide] (AMRESCO) solution was added to wells at a final concentration of 0.45 mg mL^{-1} per the manufacturer's protocol. Absorbance was measured at 570 nm (reference 650 nm) and recorded using the Safire II Multi-Mode Microplate reader (Tecan, Männedorf, Switzerland). Percentage cell viability was calculated as [sample absorbance − media background absorbance]/[control absorbance − media background absorbance] × 100. At least three independent biological replicates were performed per PLA IL. HCl solutions (pH 4–7.5) were also tested following the same protocol.

Statistical analysis

All statistical analyses were performed using Prism 9.0 software (GraphPad, San Diego, CA). Two-way ANOVA with Bonferroni's adjustment was used to compare MTT data between PLA ILs and untreated controls. The analysis was conducted on at least three independent biological replicates and displayed as mean with standard error of the mean (SEM). P values <0.05 were considered statistically significant.

Results

D-PLA as well as L-PLA can be converted to viscous ILs using biocompatible cations

We used previously reported metathesis reaction conditions to enable interaction between choline bicarbonate and D- or L-PLA, at different ratios. As anticipated, choline bicarbonate and D- or L-PLA neutralised each other yielding viscous liquids and carbon dioxide gas as a by-product (Scheme 1A and B). After complete drying in a vacuum oven for 48 h, Chol : D-PLA and Chol : L-PLA (both in the ratio of 1 : 1 and 1 : 2) remained as clear viscous ILs. The Car : PLA ILs were synthesised by mixing carnitine base and D- or L-PLA in methanol as previously reported for carnitine ILs (Scheme 1C). Car : D-PLA and Car : L-PLA were also found to be clear viscous ILs.

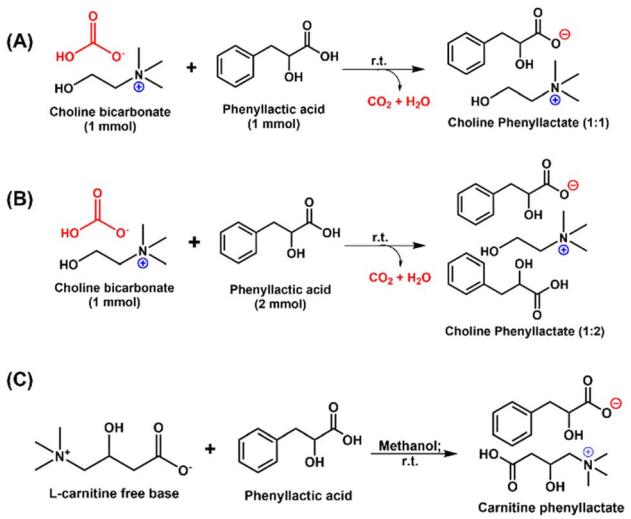

Scheme 1 Synthesis scheme for the development of (A) Chol : D-PLA (1 : 1) and Chol : L-PLA (1 : 1), (B) Chol : D-PLA (1 : 2) and Chol : L-PLA (1 : 2), and (C) Car : D-PLA (1 : 1) and Car : L-PLA (1 : 1).

Spectroscopic, chromatographic, and thermal characterization techniques confirmed the formation and purity of PLA ILs

To confirm the formation and purity of PLA ILs, we used FT-IR spectroscopy, HPLC, ^{1}H NMR spectroscopy, and thermal techniques. The FT-IR spectrum of D-PLA or L-PLA showed a sharp peak at ~3400 cm^{-1} and a broad peak at ~2900 cm^{-1} corresponding to the hydroxyl –OH stretch and carboxylic acid –OH stretch respectively (Fig. 1). The spectra also demonstrated the peak of carboxylic acid (–C=O) stretch at 1726 cm^{-1}. Similarly, the FT-IR spectrum of carnitine showed the hydroxyl stretching and bending at 3388 and 1580 cm^{-1}, while the peak at 1687 cm^{-1} corresponds to the carboxylic acid (–C=O) stretch. Upon the formation of Chol : D-PLA (1 : 1) and Chol : L-PLA (1 : 1) ILs, the carboxylic acid stretch of PLA disappeared, whereas the hydroxyl stretching peak of PLA and choline merged. The new

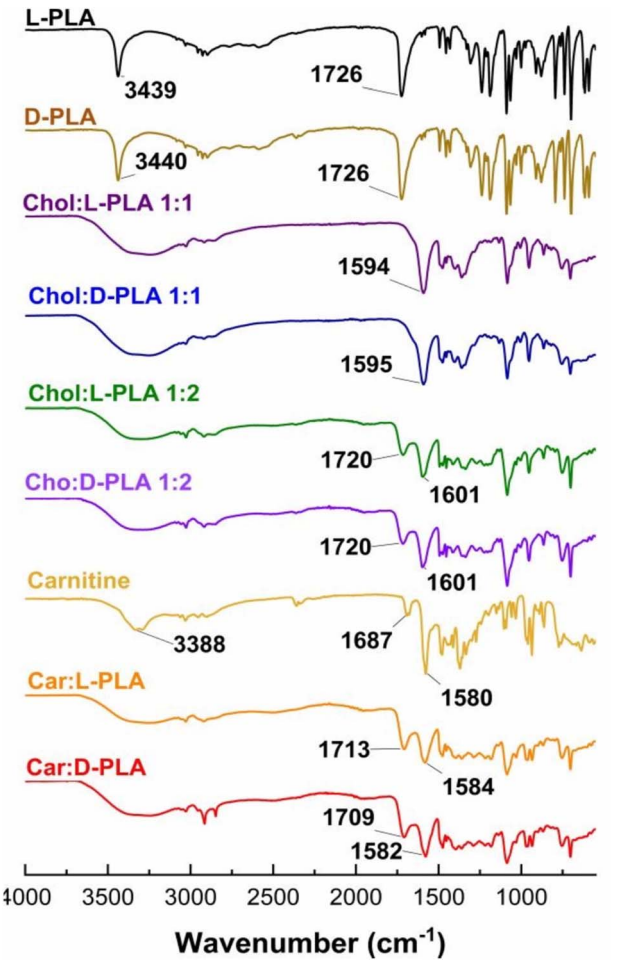

Fig. 1 FTIR characterisation of D- and L-PLA, carnitine and its corresponding ILs. The FTIR spectra of PLA ILs show disappearance of or significant shifts in –C=O stretch of PLA indicating its interaction with the choline and carnitine base.

peak at ~1595 cm^{-1} corresponds to the –OH bending of choline. The FT-IR spectrum of Chol : D-PLA (1 : 2) and Chol : L-PLA (1 : 2) showed the peak of carboxylic acid stretch because of an extra mole of PLA but with a significant shift (1720 cm^{-1}). Similarly, carnitine-based PLA ILs demonstrated a significant shift in the peaks corresponding to –C=O stretching and –OH bending (Fig. 1). The FT-IR observations indicate the electrostatic interactions between D- or L-PLA and biocompatible cations.

^{1}H NMR spectrum of D-PLA, L-PLA, Chol : D-PLA, Chol : L-PLA, Car : D-PLA, and Car : L-PLA confirmed the formation of ion pair (Fig. 2). The signal from the –COOH of the D-PLA (12.30 ppm) as well as L-PLA (12.47 ppm) disappeared in the NMR spectra of all PLA ILs (Fig. 2A and B) confirming the electrostatic interaction between PLA and counter ions (Fig. 2A and B). The hydroxyl proton shifts of D-PLA and L-PLA (5.30 ppm) showed significant displacement in all PLA ILs. Additionally, the proton adjacent to the hydroxyl group of the PLA (–CH : 2) showed prominent displacement in the NMR spectra of all PLA ILs. This could be due to the hydrogen bonding and steric hindrance of the corresponding counterions. We confirmed the purity of the synthesised PLA ILs using HPLC (Fig. S13†).

Thermogravimetric analysis (TGA) was used to determine the thermal stability of pure PLA, carnitine, and PLA ILs, and the temperature corresponding to the 5% loss of the total mass of the sample was measured ($T_{5\%}$). The $T_{5\%}$ was reached at 156.07 °C for the pure L-PLA compound, while for the pure carnitine free-base, it was at 189.9 °C (Fig. 3A and B). The $T_{5\%}$ for Car : L-PLA (1 : 1) and Car : D-PLA (1 : 1) ILs was at 82.38 °C and 76.1 °C, respectively. The Chol : D-PLA (1 : 1) and Chol : L-PLA (1 : 1) IL $T_{5\%}$ were almost similar, 94.3 °C and 93.72 °C, respectively. However, $T_{5\%}$ values increased to 198.94 °C and 159.59 °C for Chol : D-PLA (1 : 2) and Chol : L-PLA (1 : 2) respectively. Thus, carnitine-based PLA (1 : 1) and choline-based PLA (1 : 1) ILs showed a decrease in thermal stability while Chol : PLA ILs (1 : 2) demonstrated improvement.

The differential scanning colorimetric (DSC) analysis of D-PLA, L-PLA, carnitine free base, and all PLA ILs is shown in Fig. 3C. The DSC thermogram of both L- and D-PLA showed sharp endotherm at 125 °C and 124.4 °C respectively, which confirms their crystallinity. The thermograms of carnitine-based ILs and choline-based ILs of PLA did not show the melting peaks of PLA. All PLA ILs showed a slight change in baseline [~70 °C in Car : PLA (1 : 1), ~130 °C in Chol : PLA (1 : 2) and ~90 °C in Chol : PLA (1 : 1)], corroborating the TGA data of

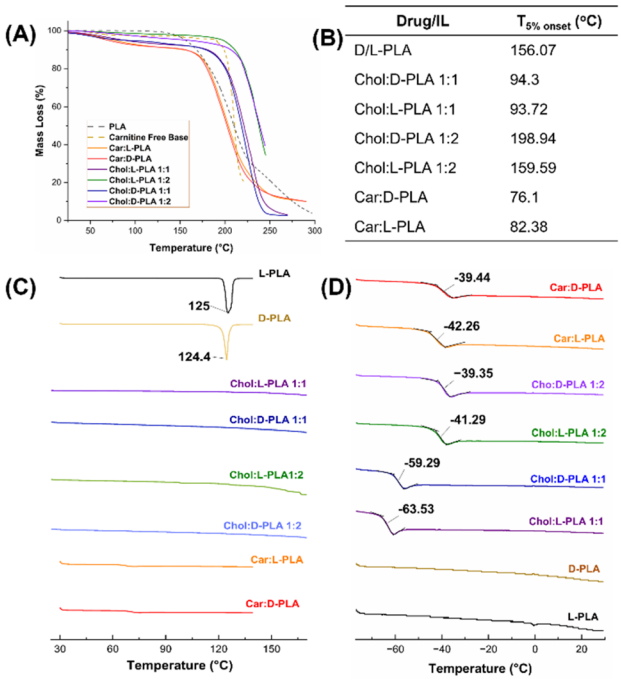

Fig. 3 (A) Thermogravimetric analysis (TGA) of PLA, carnitine and various PLA ILs. Chol : D-PLA (1 : 2) and Chol : L-PLA (1 : 2) displayed higher thermal stability compared to pure PLA. (B) $T_{5\%}$ (onset temperature at 5% mass loss) of PLA and its ILs observed in the TGA analyses. (C) Differential scanning calorimetry (DSC) thermogram of D- and L-PLA and its ILs. The thermal behaviour of samples was recorded upto the temperature corresponding to their $T_{5\%}$. The disappearance of PLA melting peak in PLA ILs indicates the amorphization of PLA because of the interaction between PLA and counterions. (D) Determination of the glass transition temperature (T_g) of D- and L-PLA and its choline/carnitine based ILs.

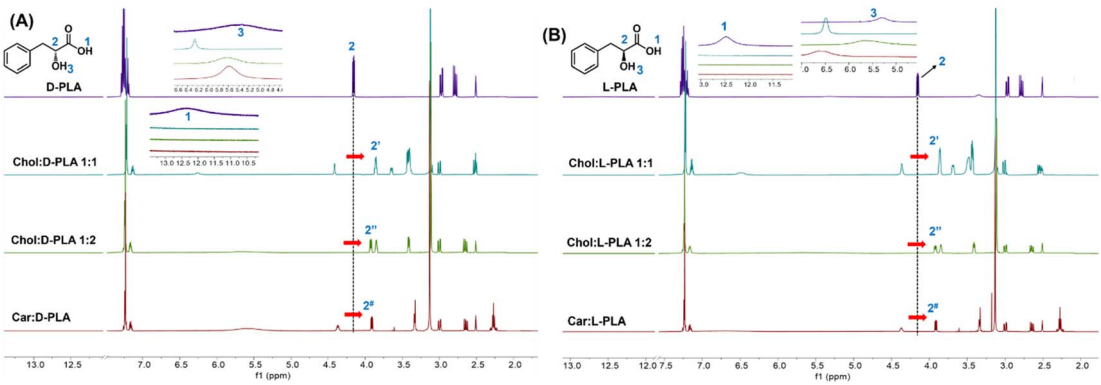

Fig. 2 ^{1}H NMR spectra of D-PLA ILs (A) and L-PLA ILs (B) showed the disappearance of carboxylic acid proton shift of PLA (–COOH : 1) and significant displacement of hydroxyl proton (–OH : 3) and proton adjacent to a hydroxyl group (–CH : 2) of PLA was observed in the ^{1}H NMR spectrum of PLA ILs. This indicates the ionic interaction between D and L-PLA and counterions.

these ILs (Fig. 3A and B). The DSC thermograms of PLA ILs suggest the total distortion of PLA crystalline lattice and conversion into the amorphous form.

The glass transition (T_g) temperatures of Chol : D-PLA (1 : 1) and Chol : L-PLA (1 : 1) ILs were −63.53 °C and −59.29 °C, respectively (Fig. 3D) whereas the T_g temperatures for Chol : D-PLA (1 : 2) and Chol : L-PLA (1 : 2) ILs drastically increased to −41.29 °C and −39.35 °C, respectively, suggesting the differential amorphicity because of extra moles of PLA in choline-based IL. The T_g temperature for Car : D-PLA (1 : 1) and Car : L-PLA (1 : 1) compounds were almost similar to that of Chol : D-PLA (1 : 2) and Chol : L-PLA (1 : 2) ILs (Fig. 3D). The appearance of the T_g curve in all PLA ILs confirms the total amorphization of crystalline PLA.

X-Ray diffractogram of D- and L-PLA, carnitine, and choline-based ILs is shown in Fig. 4. Pure D-PLA showed sharp diffraction peaks at 2θ of 15, 18, 21, and 26° and L-PLA displayed peaks at 15, 18, 21, 24, and 26°, confirming their crystallinity. Similarly, L-carnitine demonstrated sharp diffraction peaks at 9, 19, 22, and 28°. The absence of diffraction peaks in the X-ray diffractogram of all PLA ILs (Fig. 4) proves that choline and carnitine successfully converted PLA into amorphous form.

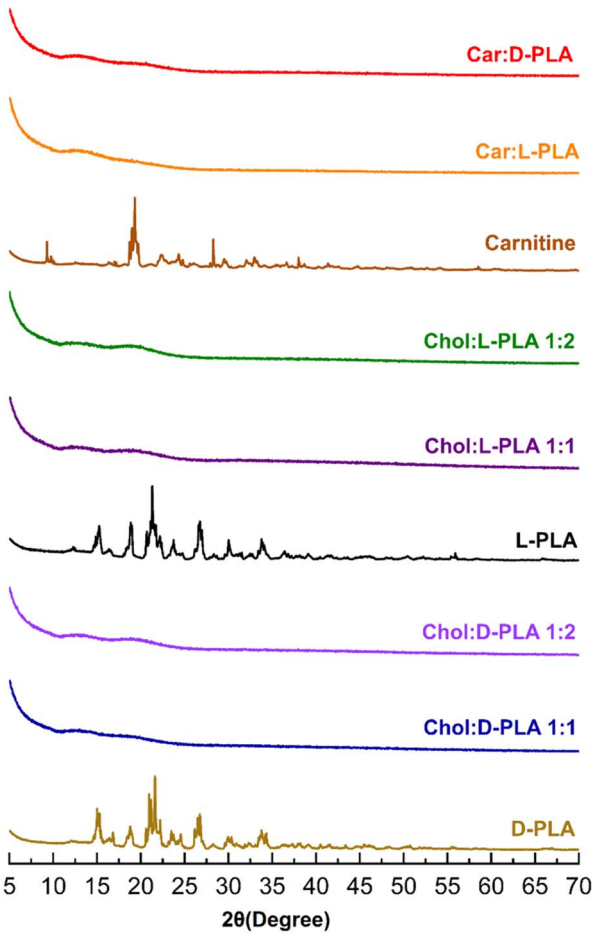

Fig. 4 X-ray diffractogram of D- and L-PLA, carnitine free base, and its corresponding ILs. All the PLA ILs showed the absence of characteristic X-ray diffraction peaks corresponding to PLA and carnitine which confirms the formation of IL with full amorphization.

PLA ILs demonstrate high water solubility

The experimental saturation solubility of D- and L-PLA in water was found to be 33.15 ± 0.44 and 25.67 ± 1.02 mg mL^{-1} respectively (Table 1). On the contrary, all PLA ILs showed significantly higher aqueous solubility (Table 1) irrespective of the cation type, PLA isomer, and the ratio of PLA to cation. As expected, upon formation of an ionic bond with hydrophilic counterion like choline at a 1 : 1 molar ratio, the solubility of the resulting IL of both the isomers of PLA increased significantly (Table 1). The pH of PLA ILs containing a 1 : 1 molar ratio of choline and PLA showed alkaline pH (~9) whereas Chol : D-PLA (1 : 2), Chol : L-PLA (1 : 2), Car : D-PLA (1 : 1) and Car : L-PLA (1 : 1) ILs showed acidic pH (~4).

Low concentrations of PLA ILs are not cytotoxic to cervical epithelial cells

To determine the cytotoxic effects of the synthesised PLA ILs on the cervical epithelium, cervical epithelial cell morphology was visualised by crystal violet staining following treatment with Chol : D-PLA (1 : 1), Chol : L-PLA (1 : 1), Chol : D-PLA (1 : 2), Chol : L-PLA (1 : 2), Car : D-PLA (1 : 1), and Car : L-PLA (1 : 1) ILs. Untreated cells maintained a healthy, confluent monolayer with a healthy ratio of cytoplasm to nuclear cellular content. Following 24 h treatment with Chol : D-PLA (1 : 1) or Chol : L-PLA (1 : 1), no morphological changes were observed even at 100 mM (Fig. 5A and S14A†). However, following treatment with Chol : PLA (1 : 2) and Carn : PLA (1 : 1) ILs, decreased cellular density and increased cellular damage were observed at higher concentrations of 100 to 25 mM (Fig. 5B, C and S14B and C†). At lower concentrations of 12.5 to 3.125 mM, no morphological changes were observed, and cell appearance was similar to untreated controls. Car : D-PLA (1 : 1) and Car : L-PLA (1 : 1) ILs, however, marginally reduced cell confluency at 12.5 mM compared to Chol : D-PLA (1 : 2) and Chol : L-PLA (1 : 2). Cervical epithelial monolayers were also treated with hydrochloric acid (HCl) control solutions with pH ranging from 4 to 7.5 for 24 h and stained with crystal violet to observe the effect of pH on cell morphology. At low pH, similar morphological changes to high concentrations of PLA IL were observed (Fig. 5D and S14D†). This largely indicates that the observed morphological changes at high PLA IL concentrations were likely due to the low pH of the solutions and that, at lower concentrations, PLA ILs cause no morphological changes to cervical epithelial cells.

Table 1 Solubility of D/L-PLA and their ILs in water. Data expressed as mean ± standard deviation (S.D.); $n = 3$

Compound	Solubility in water (mg mL^{-1})	pH
L-PLA	25.67 ± 1.02	3.2 ± 1.6
D-PLA	33.15 ± 0.44	2.9 ± 1.2
Chol : L-PLA (1 : 1)	1379.5 ± 1.6	8.78 ± 1.4
Chol : D-PLA (1 : 1)	1493.8 ± 2.5	9.02 ± 1.7
Chol : L-PLA (1 : 2)	1253.1 ± 1.8	3.87 ± 2.5
Chol : D-PLA (1 : 2)	1483.7 ± 1.5	3.86 ± 1.9
Car : L-PLA	1534.2 ± 1.3	3.87 ± 0.4
Car : D-PLA	1461.4 ± 1.5	3.96 ± 0.3

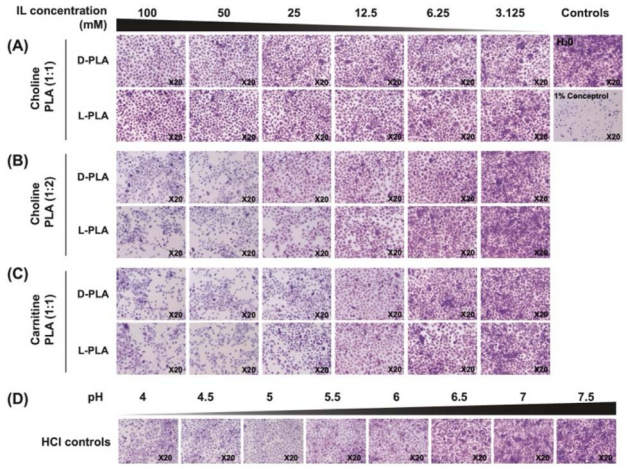

Fig. 5 PLA ILs cause no morphological changes to human cervical epithelial cells at low concentrations (≤12.5 mM). Microscopy images, at ×20 magnification, of crystal violet stained cervical epithelial (A2EN) cells, grown as monolayers, following 24 h treatment with varying concentrations of (A) Chol : D-PLA (1 : 1) and Chol : L-PLA (1 : 1), (B) Chol : D-PLA (1 : 2) and Chol : L-PLA (1 : 2), and (C) Car : D-PLA (1 : 1) and Car : L-PLA (1 : 1), and (D) HCl control solutions. Deionised water and 1% conceptrol were used as negative and positive controls, respectively.

To quantify changes in cell viability following PLA IL treatment, we conducted MTT assays. MTT is only metabolised by actively proliferating cells, thus is used to measure cellular metabolic activity as an indicator of cell viability. After 24 h, treatment with Chol : D-PLA (1 : 1) and Chol : L-PLA (1 : 1) ILs did not significantly reduce cervical epithelial cell viability, even at high concentrations of 50 mM (Fig. 6A). On the other hand, Chol : PLA (1 : 2) and Car : PLA (1 : 1) ILs significantly reduced cell viability at concentrations of 100 to 25 mM ($P < 0.0001$) and 100 to 12.5 mM ($P < 0.0001$), respectively (Fig. 6B and C). Following treatments of 100–50 mM Chol : PLA (1 : 2) and 100–25 mM Car : PLA (1 : 1), mean percentage cell viabilities were reduced similarly to between 0.4–4.1% and 0.5–3.6%, respectively. At 25 mM of Chol : PLA (1 : 2) and 12.5 mM of Car : PLA (1 : 1), mean percentage cell viabilities increased to approximately 27.4% and 64.4%, respectively, although were still significantly different from untreated controls ($P < 0.0001$). Interestingly, however, at lower concentrations (6.25 to 3.125 mM) of Chol : D-PLA (1 : 2) and Chol : L-PLA (1 : 2) ILs, we observed significantly increased cell viability compared to untreated controls ($P < 0.001$). This trend was also observed at 3.125 mM of carnitine-based PLA ILs, although only significantly for the L-isoform ($P < 0.01$). ILs containing L-PLA overall showed marginally greater toxicity than D-PLA. HCl controls revealed that low pH, equivalent to the pH of Chol : PLA (1 : 2) and Car : PLA (1 : 1) ILs at high concentrations, cause similar level of cytotoxicity as corresponding ILs (Fig. S15†). These findings corroborate our crystal violet staining observations and further demonstrate that choline-based PLA ILs had the least impact on cervical epithelial cells morphology and cytotoxicity, that low pH of ILs impact cell viability, and that all PLA IL formulations cause no cytotoxicity at lower concentrations.

Discussion

A dysbiotic vaginal microbiome, characterised by depletion of the optimal *Lactobacillus*-dominant community state and overgrowth of diverse anaerobes, can have a severe impact on women's health and lead to increased risk of bacterial vaginosis (BV), sexually transmitted infections (STIs), and pregnancy complications. In turn, these can cause more life-threatening consequences including gynaecological cancers, preterm birth, spontaneous miscarriage, pelvic inflammatory disease, and endometritis.[32] Current therapies for modulating the vaginal microbiome largely rely on antibiotics and antifungals to target infections, however, these are often ineffective against recurrent conditions, leading to overuse of antibiotics and contributing to the growing incidence of bacterial resistance. Several novel therapeutic approaches have therefore been proposed with promising results, including probiotics, prebiotics, biofilm disruptive agents, novel antimicrobials, and vaginal microbiota transplant (VMT).[33] We proposed that using metabolites produced by healthy constituents of the vaginal microbiome, such as PLA, would be a promising approach to modulate the vaginal microbiome, aid in restoring homeostasis, and reduce the risk of serious gynaecological and obstetric outcomes. However, these metabolites would need to be soluble and non-toxic to the cervicovaginal epithelium.

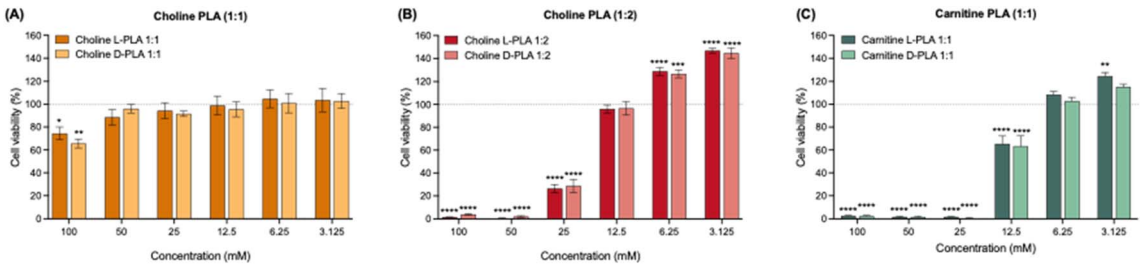

Fig. 6 PLA ILs cause no cytotoxicity to human cervical epithelial cells at low concentrations (≤6.25 mM). Percentage cell viability was determined by MTT assay following 24 h treatment of cervical epithelial (A2EN) cell monolayers with varying concentrations of PLA-ILs and pH solutions: (A) Chol : D-PLA (1 : 1) and Chol : L-PLA (1 : 1), (B) Chol : D-PLA (1 : 2) and Chol : L-PLA (1 : 2), and (C) Car : D-PLA (1 : 1) and Car : L-PLA (1 : 1). Absorbance was measured at 570 nm (650 nm reference). Percentage cell viability was calculated relative to untreated control (100%) and plotted as mean ± SEM, using at least 3 independent experiments per compound. Significance was determined using two-way ANOVA with Bonferroni's adjustment. Asterisks indicate significance: ****$P < 0.0001$; ***$P < 0.001$; **$P < 0.01$; *$P < 0.05$.

PLA has numerous promising antibacterial, antifungal, and immunomodulatory properties but previous studies indicated that a high concentration of PLA is required to elicit these effects. Although the equilibrium solubility of D- and L-PLA in water is > 25 mg mL^{-1} (Table 1), the kinetic solubility of D- and L-PLA is considerably lower, and our preliminary studies and previous reports[27] show that toxic solvents such as DMSO and ethanol are necessary to solubilise PLA. However, DMSO or ethanol, due to their toxicity to human epithelial cells, would not be appropriate for intravaginal delivery. Hence, a strategy that uses biocompatible ingredients to yield high solubility of PLA is needed to maintain its safety for use on human mucosal surfaces.

In recent years, ionic liquids (ILs) have been extensively researched for their use in biomedicine, due to their ability to solubilise compounds for drug formulations or drug delivery systems. Overall, ILs enable greater solubility, permeability, and bioavailability of compounds. Although previously some ILs have demonstrated toxic properties,[34] this has been combated through formulating ILs with more biocompatible counterions, namely those of natural source.[35] In the past decade, ILs based on endogenous cation, choline, and organic acids have been explored for numerous drug delivery applications due to their excellent solubility, biocompatibility, and permeability across various biological membranes including epithelial surfaces. For example, choline-based ILs were identified to have enhanced solubility and cause lower cytotoxicity to human keratinocyte cells, compared to imidazole-based ILs, amongst the most studied ILs, and were concluded as more suitable for incorporation into topical drug formulations.[36] Further, they have been investigated as drug delivery systems for anticancer agents[37] and shown to significantly enhance the solubility of ibuprofen,[38] both without inducing cytotoxicity.

While choline-based biocompatible ILs are being widely explored for drug delivery, other biocompatible cations such as carnitine have been minimally explored for the synthesis of biocompatible ILs. Carnitine exists as two biologically active enantiomers, L- and D-carnitine, of which only L-carnitine is endogenously synthesised by the human liver, kidneys, and brain. Although carnitine-based ILs are less studied, one report showed they can be combined with ascorbic acid and benzoic acid derivatives to enhance solubility in water and form antioxidant ILs.[39] Carnitine-based ILs have also been utilised to synthesise herbicidal ionic liquids with low toxicity and enhanced biodegradability,[40] and to stabilise and solubilise antimicrobial eye drops.[41] Hence, we envisaged that endogenous cations, choline and L-carnitine, could be readily used to transform D- and L-PLA into ILs. Our previous studies show that the biocompatible anion used for the synthesis of ILs impacts the solubility and *in vitro* cytocompatibility of ILs.[30,42] However, the effect of biocompatible cation used for the IL synthesis on the physicochemical properties and cytocompatibility of ILs was not explored. Hence, we focused on the evaluation of the physicochemical properties and cytocompatibility of choline or carnitine-based PLA ILs.

Using previously reported methods, we were able to convert both D- and L-PLA into viscous ILs using equimolar quantities of choline bicarbonate or L-carnitine. The NMR spectra of resulting D- or L-PLA ILs showed the absence of carboxylate proton of PLA and significant shifts in other protons indicating the ionic interaction between D- or L-PLA and cations. We used several other characterisation techniques to confirm the formation and purity of PLA ILs. As anticipated, the D- or L-PLA ILs containing a 1 : 1 molar ratio of choline or carnitine showed >50-fold higher aqueous solubility compared to pure D- or L-PLA. However, the pH values of Chol : L-PLA (1 : 1) and Chol : D-PLA (1 : 1) were ~9 mainly due to the high basicity of choline (pK_a : 11.2). On the contrary, Car : PLA (1 : 1) ILs showed pH value of ~4 due to its zwitterionic nature and low pK_a (3.8) of carnitine. For effective intravaginal delivery, the vaginal formulations should maintain a pH akin to the acidic milieu in the vagina (pH ~ 4–4.5). Hence, Car : PLA (1 : 1) ILs were deemed to be suitable for further evaluation. However, to increase the acidity of choline-based PLA ILs for intravaginal applications, we decided to synthesise PLA ILs containing choline and D- or L-PLA at a 1 : 2 molar ratio. The addition of another mole of D- or L-PLA to choline-based ILs considerably impacted the thermal stability and glass transition temperature of the Chol : PLA (1 : 2) ILs. Furthermore, the inclusion of an additional mole of PLA in the ILs significantly reduced the pH from ~9 to a pH value of 4 making it suitable for intravaginal application while maintaining the high water solubility of PLA.

The PLA ILs of similar low pH, Car : PLA (1 : 1) and Cho : PLA (1 : 2), differed only minimally in their *in vitro* cytotoxicity analysis, in which slightly higher concentrations of Cho : PLA (1 : 2) were tolerated by cervical epithelial cells compared to Car : PLA (1 : 1). This indicates that either choline is a less toxic counterion than carnitine or that a higher ratio of PLA aids in reducing cytotoxicity. ILs with higher pH, Cho : PLA (1 : 1) ILs, were considerably less cytotoxic than both Cho : PLA (1 : 2) and Car : PLA (1 : 1) ILs. This pattern closely corresponded with cytotoxicity observed with hydrochloric acid pH controls, indicating that a more neutral pH results in reduced cytotoxicity, and that the acidic pH of Car : PLA (1 : 1) and Cho : PLA (1 : 2) may be the ultimate explanation for their cytotoxicity at high concentrations. Since a lower pH of ILs is preferred for use in the vaginal microenvironment, future formulations of PLA ILs could involve their development into gels to help reduce the impact of pH on the epithelium.

Interestingly, at low concentrations of Cho : PLA (1 : 2) ILs, cell viability was significantly enhanced compared to untreated controls. This was not observed for Cho : PLA (1 : 1), and only marginally for Car : L-PLA (1 : 1), further supporting that a greater PLA ratio reduces cytotoxicity and may even enhance epithelial cell growth. Physiological concentrations of lactic acid produced by vaginal *Lactobacilli* sp. were recently shown to enhance cervicovaginal epithelial barrier integrity by promoting intracellular tight junction protein expression,[43] and have also demonstrated anti-inflammatory activity.[44] Although these observations were not specific to aromatic lactic acids or PLA, this provides a potential mechanism in which PLA ILs could enhance the cervicovaginal epithelium as observed in the present study. Future experiments utilising our human three-dimensional (3D) cervical epithelial cell model,[19,45] that

recapitulates the characteristics of human cervical epithelium, could aid in elucidating the immunomodulatory and barrier-protective role of PLA ILs in the cervicovaginal microenvironment. Additionally, further cytotoxicity testing utilising advanced *in vitro* models or a rabbit *in vivo* model will confirm the safety of the PLA IL compounds for intravaginal use and help identify the safest formulation for further development. Use of the 3D model would also enable assessment of the antibacterial, antifungal, and antiviral activities of the PLA ILs following colonisation of the epithelial cells with commensal vaginal microbiota or infection with pathogenic microorganisms, including common vaginal STIs, fungi, and viruses.

Beyond the use of PLA ILs as vaginal microbiome modulators, they could be highly applicable in other areas of biomedical research due to the vast protective and immunomodulatory properties of PLA. In a mouse model, it was found that PLA upregulates intestinal peroxisome proliferator-activated receptor γ (PPAR-γ) activity, a lipid metabolism regulator to protect against metabolic dysfunction, generated by early-life antibiotic exposure and high-fat diet, and ultimately prevent early-life obesity.[46] Aromatic lactic acids, including PLA, produced by *Bifidobacterium* species in the infant gut can modulate gut health and immune development.[47] Similarly, PLA was found to protect against *Salmonella enterica* serovar Typhimurium-induced colitis in mice by regulating intestinal microbiota, increasing the abundance of *Lactobacillus*, and eliminating inflammation.[18] Furthermore, PLA was previously patented as a skin-protecting ingredient to reduce skin wrinkles,[16] highlighting its potential role in the cosmetic industry. When synthesised into a highly soluble, bioavailable IL, these properties of PLA could now be fully exploited for pharmaceutical use.

Conclusion

The quaternary biocompatible cations, choline, and carnitine, could be used to transform phenyllactic acid into highly water soluble phenyllactic acid ionic liquids using a salt metathesis reaction. The formation of phenyllactic acid ionic liquids was confirmed using spectroscopic and chromatographic techniques. The structure and the ratio of the cation to phenyllactic acid and the conformation of phenyllactic acid impacted the solubility, pH, and cytocompatibility to cervical epithelial cells. As previously stated, future studies are required to fully elucidate the effects of phenyllactic ionic liquids on the cervicovaginal microenvironment, including *in vitro* studies on vaginal epithelial cells, 3D cell models, as well as clinical studies to fully determine the safety and tolerability of phenyllactic acid ionic liquid of interest.

Author contributions

M. M. H.-K. and A. D. conceived, designed, and supervised the study. Y. S., I. T., and S. M. performed IL synthesis and physicochemical experiments. P. C. and P. Ł. performed IL toxicity experiments. All authors analysed and interpreted the data. P. C., I. T., and Y. S. drafted the manuscript. All authors read, critically reviewed, and approved the final version of the paper.

Conflicts of interest

M. M. H.-K. is a paid consultant for Vaginal Biome Sciences and serves on the scientific advisory board for Freya Biosciences. None of this work related to, was shared with, or was licensed to this company or any other commercial entity. A. A. D, Y. S., I. T., S. M., P. C., and P. Ł. declare no competing interests.

Acknowledgements

A. A. D. would like to acknowledge support from R. K. Coit College of Pharmacy Startup Fund and NIAID grant (R21AI176907). M. M. H.-K. would like to acknowledge the UA COM-Phoenix Department of Obstetrics and Gynecology for support for P. C., and P. L. was supported by the Guiding U54 Investigator Development to Sustainability (GUiDeS) program under the award for the Partnership of Native American Cancer Prevention funded by the National Cancer Institute of the National Institutes of Health (U54CA143924).

Notes and references

1 W. Mu, S. Yu, L. Zhu, T. Zhang and B. Jiang, *Appl. Microbiol. Biotechnol.*, 2012, **95**, 1155–1163.
2 E. Dempsey and S. C. Corr, *Front. Immunol.*, 2022, **13**, 840245.
3 M. L. Neugent, N. V. Hulyalkar, V. H. Nguyen, P. E. Zimmern and N. J. De Nisco, *mBio*, 2020, **11**, e00218–20.
4 M. A. Antonio, S. E. Hawes and S. L. Hillier, *J. Infect. Dis.*, 1999, **180**, 1950–1956.
5 R. Rajanikar, B. H. Nataraj, H. Naithani, S. A. Ali, N. R. Panjagari and P. V. Behare, *Food Control*, 2021, **128**, 108184.
6 S. Siedler, R. Balti and A. R. Neves, *Curr. Opin. Biotechnol.*, 2019, **56**, 138–146.
7 V. Dieuleveux, S. Lemarinier and M. Gueguen, *Int. J. Food Microbiol.*, 1998, **40**, 177–183.
8 F. Valerio, P. Lavermicocca, M. Pascale and A. Visconti, *FEMS Microbiol. Lett.*, 2004, **233**, 289–295.
9 Y. Ning, Y. Fu, L. Hou, M. Ma, Z. Wang, X. Li and Y. Jia, *Food Res. Int.*, 2021, **139**, 109562.
10 Y.-H. Jiang, J.-P. Ying, W.-G. Xin, L.-Y. Yang, X.-Z. Li and Q.-L. Zhang, *J. Dairy Sci.*, 2022, **105**, 9463–9475.
11 P. Lavermicocca, F. Valerio, A. Evidente, S. Lazzaroni, A. Corsetti and M. Gobbetti, *Appl. Environ. Microbiol.*, 2000, **66**, 4084–4090.
12 S. M. Schwenninger, C. Lacroix, S. Truttmann, C. Jans, C. Spörndli, L. Bigler and L. Meile, *J. Food Prot.*, 2008, **71**, 2481–2487.
13 V. Dieuleveux, D. Van Der Pyl, J. Chataud and M. Gueguen, *Appl. Environ. Microbiol.*, 1998, **64**, 800–803.
14 J. Wang, J. Yoo, J. Lee, T. Zhou, H. Jang, H. Kim and I. Kim, *J. Appl. Poultry Res.*, 2009, **18**, 203–209.
15 F. J. Urban and B. S. Moore, *J. Heterocycl. Chem.*, 1992, **29**, 431–438.

16 R. J. Yu and E. J. Van Scott, *US Pat.*, 5643953A, 1997.
17 A. Peters, P. Krumbholz, E. Jäger, A. Heintz-Buschart, M. V. Çakir, S. Rothemund, A. Gaudl, U. Ceglarek, T. Schöneberg and C. Stäubert, *PLoS Genet.*, 2019, **15**, e1008145.
18 Q. Zhou, R. Gu, B. Xue, P. Li and Q. Gu, *Food Funct.*, 2021, **12**, 5591–5606.
19 P. Łaniewski and M. M. Herbst-Kralovetz, *npj Biofilms Microbiomes*, 2021, **7**, 88.
20 N. R. Jimenez, J. D. Maarsingh, P. Łaniewski and M. M. Herbst-Kralovetz, *mSphere*, 2023, **8**, e0045222.
21 J. H. Saigh, C. C. Sanders and W. E. Sanders, *Infect. Immun.*, 1978, **19**, 704–710.
22 Z. Gong, Y. Luna, P. Yu and H. Fan, *PLoS One*, 2014, **9**, e107758.
23 K. Gupta, A. E. Stapleton, T. M. Hooton, P. L. Roberts, C. L. Fennell and W. E. Stamm, *J. Infect. Dis.*, 1998, **178**, 446–450.
24 S. L. Hillier, M. A. Krohn, L. K. Rabe, S. J. Klebanoff and D. A. Eschenbach, *Clin. Infect. Dis.*, 1993, **16**, S273–S281.
25 M. Falagas, G. Betsi and S. Athanasiou, *Clin. Microbiol. Infect.*, 2007, **13**, 657–664.
26 G. Tachedjian, M. Aldunate, C. S. Bradshaw and R. A. Cone, *Res. Microbiol.*, 2017, **168**, 782–792.
27 O. Abdul-Rahim, Q. Wu, T. K. Price, G. Pistone, K. Diebel, T. S. Bugni and A. J. Wolfe, *J. Bacteriol.*, 2021, **203**, e0036021.
28 M. K. Shukla, H. Tiwari, R. Verma, W.-L. Dong, S. Azizov, B. Kumar, S. Pandey and D. Kumar, *Pharmaceutics*, 2023, **15**, 702.
29 W. Huang, X. Wu, J. Qi, Q. Zhu, W. Wu, Y. Lu and Z. Chen, *Drug Discovery Today*, 2020, **25**, 901–908.
30 Y. Sutar, S. K. Singh, S. Dhoble, J. Mali, J. Adams, T. Yadavalli, A. A. Date and D. Shukla, *ACS Infect. Dis.*, 2024, **10**, 93–106.
31 M. M. Herbst-Kralovetz, A. J. Quayle, M. Ficarra, S. Greene, W. A. Rose 2nd, R. Chesson, R. A. Spagnuolo and R. B. Pyles, *Am. J. Reprod. Immunol.*, 2008, **59**, 212–224.
32 D. H. Martin and J. M. Marrazzo, *J. Infect. Dis.*, 2016, **214**, S36–S41.
33 P. Łaniewski, Z. E. Ilhan and M. M. Herbst-Kralovetz, *Nat. Rev. Urol.*, 2020, **17**, 232–250.
34 J. Flieger and M. Flieger, *Int. J. Mol. Sci.*, 2020, **21**, 6267.
35 R. Md Moshikur, M. R. Chowdhury, M. Moniruzzaman and M. Goto, *Green Chem.*, 2020, **22**, 8116–8139.
36 T. Santos de Almeida, A. Júlio, N. Saraiva, A. S. Fernandes, M. E. M. Araújo, A. R. Baby, C. Rosado and J. P. Mota, *Drug Dev. Ind. Pharm.*, 2017, **43**, 1858–1865.
37 R. Caparica, A. Júlio, M. E. Araújo, A. R. Baby, P. Fonte, J. G. Costa and T. Santos de Almeida, *Biomolecules*, 2020, **10**, 233.
38 J. Yuan, J. Wu and T. Yin, *J. Drug Delivery Sci. Technol.*, 2020, **60**, 102037.
39 K. Czerniak and J. Pernak, *ChemistrySelect*, 2021, **6**, 1994–2001.
40 J. Pernak, M. Niemczak, Ł. Chrzanowski, Ł. Ławniczak, P. Fochtman, K. Marcinkowska and T. Praczyk, *Chem.–Eur. J.*, 2016, **22**, 12012–12021.
41 B. Grassiri, A. Mezzetta, G. Maisetta, C. Migone, A. Fabiano, S. Esin, L. Guazzelli, Y. Zambito, G. Batoni and A. M. Piras, *Int. J. Mol. Sci.*, 2023, **24**, 2714.
42 H. K. Saeed, Y. Sutar, P. Patel, R. Bhat, S. Mallick, A. E. Hatada, D.-L. T. Koomoa, I. Lange and A. A. Date, *ACS Omega*, 2021, **6**, 2626–2637.
43 D. J. Delgado-Diaz, B. Jesaveluk, J. A. Hayward, D. Tyssen, A. Alisoltani, M. Potgieter, L. Bell, E. Ross, A. Iranzadeh, I. Allali, S. Dabee, S. Barnabas, H. Gamieldien, J. M. Blackburn, N. Mulder, S. B. Smith, V. L. Edwards, A. D. Burgener, L.-G. Bekker, J. Ravel, J.-A. S. Passmore, L. Masson, A. C. Hearps and G. Tachedjian, *Microbiome*, 2022, **10**, 141.
44 I. Schwecht, A. Nazli, B. Gill and C. Kaushic, *Sci. Rep.*, 2023, **13**, 20065.
45 R. Jackson, J. D. Maarsingh, M. M. Herbst-Kralovetz and K. Van Doorslaer, *Curr. Protoc. Microbiol.*, 2020, **59**, e129.
46 C. D. Shelton, E. Sing, J. Mo, N. G. Shealy, W. Yoo, J. Thomas, G. N. Fitz, P. R. Castro, T. T. Hickman, T. P. Torres, N. J. Foegeding, J. K. Zieba, M. W. Calcutt, S. G. Codreanu, S. D. Sherrod, J. A. McLean, S. H. Peck, F. Yang, N. O. Markham, M. Liu and M. X. Byndloss, *Cell Host Microbe*, 2023, **31**, 1604.e1610–1619.e1610.
47 M. F. Laursen, M. Sakanaka, N. von Burg, U. Mörbe, D. Andersen, J. M. Moll, C. T. Pekmez, A. Rivollier, K. F. Michaelsen, C. Mølgaard, M. V. Lind, L. O. Dragsted, T. Katayama, H. L. Frandsen, A. M. Vinggaard, M. I. Bahl, S. Brix, W. Agace, T. R. Licht and H. M. Roager, *Nat. Microbiol.*, 2021, **6**, 1367–1382.